Available online at www.sciencedirect.com
ScienceDirect
International Journal of Heat and Mass Transfer 51 (2008) 4753–4758
International Journal of HEAT and MASS TRANSFER
www.elsevier.com/locate/ijhmt

Frequency response of an electrochemical probe to the wall shear stress fluctuations of a turbulent channel flow

J. Pallares *, F.X. Grau

Department of Mechanical Engineering, University Rovira i Virgili, Av. Països Catalans, 26, 43007-Tarragona, Spain

Received 18 September 2007
Available online 28 April 2008

Abstract

We analyzed numerically the frequency response of the mass transfer rates produced at the surface of an electrochemical probe to the fluctuations of the wall shear stress obtained from a direct numerical simulation of a turbulent plane channel flow at $Re_\tau = 150$. At low and high frequencies the response to the turbulent wall shear stress is in accordance with the existing relations between the amplitudes of the wall shear stress and the mass transfer rates obtained for harmonic perturbations. At intermediate frequencies the turbulent wall shear stress fluctuations produce a larger damping in comparison with the harmonic perturbations. The phase angle of the response of mass transfer rates with respect to the wall shear stress shows important deviations in comparison with the phase angle obtained with harmonic perturbations, specially at high frequencies.

Keywords: Mass transfer; Turbulence; Wall shear stress; Frequency response; Electrochemical probe

1. Introduction

Mass transfer probes are used to measure wall shear stresses in liquid flows. The probe usually consists in a small electrode mounted flush on a wall. On the surface of the electrode an electrochemical reaction occurs and the measured current can be related to the mass transfer rate by using Faraday's law. From this quantity the velocity gradient, S, at the surface of the probe and, thus, the wall shear stress, $\tau_w = \mu S$ can be obtained with the conventional design relation for mass-transfer wall gauges. The description of the theory and the experimental requirements of this measurement technique can be found in [1,2].

The use of electrochemical probes to measure the instantaneous wall shear stress in turbulent flows is conditioned by two requirements. First, the measurement of the current obtained is related to the spatially averaged mass transfer rates on the surface of the probe and consequently the dimension of the probe has to be small enough to capture the local wall shear stress fluctuations produced by the near wall flow structures. On the other hand, the time response of the mass transfer rates to a fluctuating flow field is associated with the capacitance effect of the concentration boundary layer, especially to the high frequency fluctuations. The time response of electrochemical probes has been determined experimentally in fully developed laminar pipe flows with a time-varying sinusoidal pressure gradient [3] and in rotating disk flow with a time-varying sinusoidal rotation rate [4]. These harmonic perturbations generate time evolutions of the wall shear stress with a controlled frequency and the measurement of the time response of the mass transfer rates allows the determination of the frequency response of the probe.

It is known that for low-frequency flow perturbations the analytical quasi-steady-state solution of the mass boundary layer equation, correctly describes the time response of the mass transfer rates, because the instantaneous mass transfer rate can be related to the instantaneous wall shear stress by the same equation as for steady flow. For high frequency fluctuations of the wall shear stress

* Corresponding author. Tel.: +34 977 559 682; fax: +34 977 559 691.
E-mail address: jordi.pallares@urv.cat (J. Pallares).

0017-9310/$ - see front matter © 2008 Elsevier Ltd. All rights reserved.
doi:10.1016/j.ijheatmasstransfer.2007.10.043

Nomenclature

A	amplitude
C	concentration (mol m^{-3})
D	mass diffusion coefficient (m s^{-2})
f	frequency (s^{-1})
k	convective mass transfer coefficient (m s^{-1})
L	length (m)
R	autocorrelation
Re_τ	Reynolds number ($Re_\tau = u_\tau \delta/\nu$)
S	velocity gradient (s^{-1})
Sc	Schmidt number ($Sc = \nu/D$)
Sh	Sherwood number ($Sh = k\ L_p/D$)
t	time (s)
u, v, w	Cartesian velocity components (m s^{-1})
u_τ	friction velocity, $u_\tau = (\tau_w/\rho)^{1/2}$, (m s^{-1})
W	spectral density function
x, y, z	Cartesian coordinates (m)

Greek symbols

Δ	increment
Γ	Gamma function
δ	channel half width (m)
μ	dynamic viscosity (kg m^{-1} s^{-1})
ν	kinematic viscosity (m s^{-2})
θ	phase angle
ρ	density (kg m^{-3})
τ_w	wall shear stress (N m^{-2})

Superscripts and subscripts

b	bulk
p	probe
rms	root-mean-square
w	wall
+	wall scaling
*	non-dimensional quantity
‘	fluctuation
$\langle\ \rangle$, −	time-averaged quantity

the capacitance effect of the mass transfer boundary layer produces damped fluctuations of the mass transfer rates. Since the frequency cutoff for which the quasi-steady-state can be considered to be valid is rather low owing to the large value of the Schmidt number in liquids, the determination of the transfer function has been the objective of several studies. The transfer function that relates the power spectral density of the fluctuations of the averaged mass transfer rate over the probe surface and that of the fluctuations of the velocity gradient at the wall has been reported by Desloius et al. [4], Py [5] and Mitchell and Hanratty [6] and Fortuna and Hanratty [7]. The expressions of the transfer function were obtained considering that the fluctuating velocity gradient is given as a harmonic function and by solving a linearized version of the unsteady part of the mass transfer balance. Mao and Hanratty [8–10] used an inverse method to take into account the non-linearity. These authors measured the time evolution of the mass transfer rates generated on small probes in turbulent pipe flows. The velocity gradient at the wall obtained with the quasi-steady-state solution of the mass boundary layer equation was corrected by solving iteratively the mass transport equation until the mass transfer rates obtained numerically were coincident with those measured.

In this study the frequency response of a mass transfer probe to a fluctuating wall shear stress transfer of a turbulent plane channel flow has been determined by solving numerically the complete differential unsteady mass transfer balance using the time evolution of the wall velocity gradient extracted from a direct numerical simulation (DNS) of a turbulent channel flow. To the authors' knowledge, there is no previous study that examines numerically the frequency response of mass transfer probes by using a signal of the wall shear stress that contains the intrinsic properties of the real turbulent wall shear stress, as for example its characteristic power spectra and probability density function. The information extracted from this analysis can be useful to improve the measurement of the instantaneous wall shear stress using the electrochemical technique.

2. Physical model

The physical model and the coordinate system are shown in Fig. 1. It is assumed that the mass transfer probe is flush mounted on a wall of a plane channel. The two walls of the channel are separated a distance 2δ. The fully developed flow in the channel is driven by a constant pres-

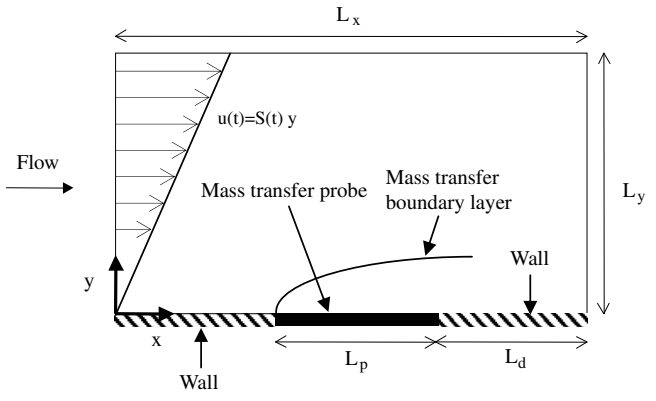

Fig. 1. Physical model.

sure gradient along the streamwise direction. The Reynolds number based on the bulk velocity and the distance between the walls is $Re = 4570$ and that based on the friction velocity and the channel half width is $Re_\tau = 150$. The concentration of the reacting electrolyte is constant outside the mass transfer boundary layer and the Schmidt number is set to 1000, typical in liquids. The physical properties of the fluid are considered constant. The electrochemical reaction occurring on the probe is assumed to be fast enough to consider the concentration of the reacting electrolyte to be zero on the probe.

The streamwise dimension of the probe is $L_p = 0.01\delta$, $L_p^+ = 1.5$ in wall units. Fig. 2 shows the streamwise (Fig. 2a) and spanwise (Fig. 2b) autocorrelations of the fluctuations of the streamwise component of wall shear stress computed from the DNS database. It can be seen that the autocorrelations agree with those predicted by the DNS of Jeon et al. [11] plotted in Fig. 2 with symbols. Fig. 2a indicates that the correlation of the fluctuations of the wall shear stress on the leading and the trailing edges of the probe considered is very close to 1. Consequently, the length of the probe is small enough to reasonably assume that the wall shear stress is constant over the streamwise extension of the computational domain of dimension $L_x = 0.02\delta$ (i.e. τ_w does not depend on x). On the other hand, the vertical dimension of the computational domain, $L_y = 0.004\delta$ ($L_y^+ = 0.6$) can be considered small enough to assume a linear variation of the instantaneous streamwise velocity component along the vertical direction (i.e. $u = Sy$). These two assumptions allow for the vertical velocity component to be neglected (i.e. $v = 0$).

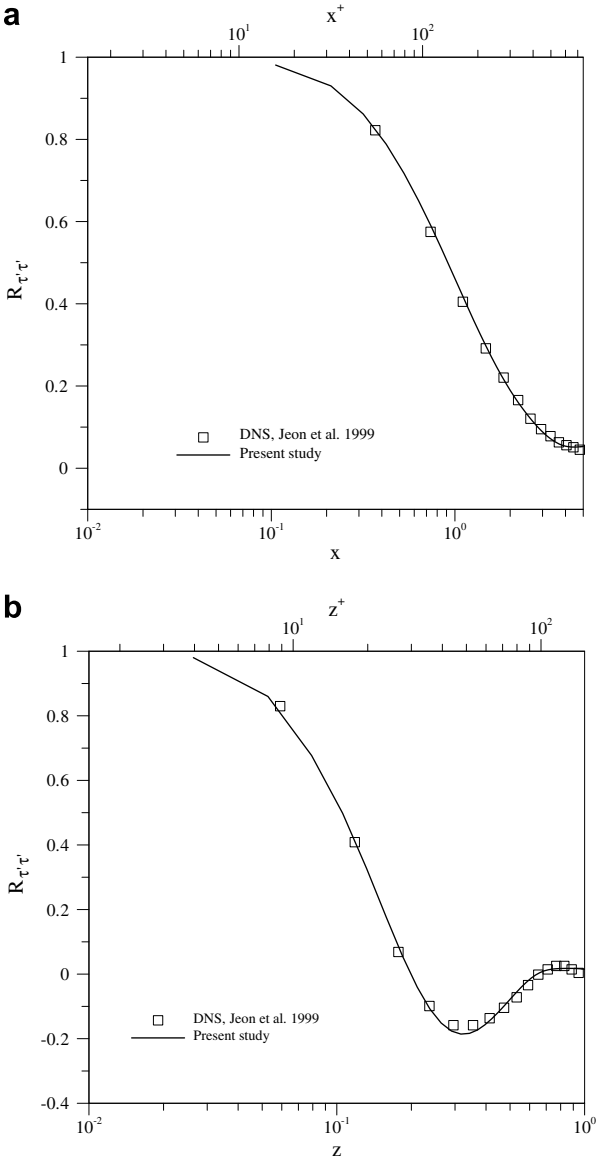

Fig. 2. Streamwise (a) and spanwise (b) autocorrelations of the wall shear stress.

The spanwise autocorrelation of the fluctuations of the wall shear stress shows that the two-dimensional approach (i.e. τ_w does not depend on z) can be considered representative for a rectangular probe with aspect ratio L_z/L_p of about three. As shown in Fig. 2b, for a probe with this aspect ratio the correlation between the fluctuations of the wall shear stress at the two edges of the probe separated a distance $3L_p$ is 0.96. It should be noted that the two-dimensional approach is also based on the assumption that the thickness of the concentration boundary layer is small enough compared to the width L_z of the electrode so that mass diffusion in the spanwise direction can be neglected. The results presented in the next sections show that the thickness of the concentration boundary layer is about 0.06 the width of a rectangular probe of aspect ratio $L_z/L_p = 3$.

Note also that the size of the computational domain $L_x^+ = 1.5$ $L_y^+ = 0.6$ is comparable to the usual grid size near the wall used in DNS of turbulent channel flows. The typical grid sizes near the wall of DNSs are about $\Delta x^+ \approx 10$–15, $\Delta y^+ \approx 0.05$–0.5 and $\Delta z^+ \approx = 4$–7. This indicates that the two-dimensional hypothesis and the consideration of a uniform wall shear stress on the probe are reasonable, for the flow conditions of the simulation.

3. Mathematical model

The above hypotheses allow writing the two-dimensional mass transfer equation (Eq. (1)) to model the relation between the wall shear stress and the mass transfer rates on an electrochemical probe mounted on a wall of the channel. In fact, Eq. (1) is the conventional approach used by previous authors [4–7] to obtain analytically the relation between the wall shear stress and the mass transfer rates.

$$\frac{\partial C^*}{\partial t^*} + S^* y^* \frac{\partial C^*}{\partial x^*} = \frac{1}{Re_\tau Sc}\left(\frac{\partial^2 C^*}{\partial x^{*2}} + \frac{\partial^2 C^*}{\partial y^{*2}}\right) \quad (1)$$

In Eq. (1), $(S^* y^*)$ is the streamwise velocity component (u^*), which is assumed to vary linearly with the vertical coordinate. Eq. (1) has been non-dimensionalized with

the channel half width (δ) and the averaged friction velocity ($u_\tau = (\tau_w/\rho)^{1/2}$) as the length and velocity scales. The resulting non-dimensional parameters are the Reynolds and the Schmidt numbers defined as, $Re_\tau = u_\tau\delta/\nu$ and $Sc = \nu/D$, respectively. The non-dimensional concentration is defined as $C^* = C/C_b$. It should be noted that the existing theoretical and numerical studies usually neglect the streamwise diffusion term according to the conventional boundary layer hypothesis. The consideration of this term in Eq. (1) modifies the concentration distribution predicted by the Leveque solution (see for example Deslouis et al. [4]) near the leading and trailing edges of the probe.

Eq. (1) has been solved numerically with a second order accuracy finite volume code, in the 2D computational domain sketched in Fig. 1 using the time evolution of S extracted from a DNS of a fully developed plane channel flow. The database of the wall shear stress contains the time evolution during 25 large-eddy turn over times ($t = 25\ \delta/u_\tau$) of the three components of the velocity vector and the pressure in 121×121 grid nodes located at $y^+ = 0.5$. The instantaneous wall shear stresses were computed assuming a linear variation of the instantaneous streamwise velocity component within the distance between the first near-wall grid node and the wall. The period of non-dimensional time recorded is about 50 times the integral time scale of the wall shear stress evolution. The details of the numerical techniques used for the DNS of the plane channel flow, as well as a detailed comparison of this simulation with those available in the literature can be found in Fabregat [12]. Recently, this database has been used to educe near-wall flow structures responsible for large fluctuations of wall shear stress [13].

The diffusion and the advection terms in Eq. (1) have been discretized in a non-uniform finite volume grid with the centered scheme and the time integration was performed with the Crank-Nicolson scheme.

The dimensions of the computational domain indicated in Fig. 1, are $L_y = 0.004\delta$, $L_p = 0.01\delta$, $L_d = 0.005\delta$, $L_x = 0.02\delta$. The boundary conditions for C^* are, $C^* = 0$ at the probe surface (i.e. at $0 < x^* < 0.01$), according to the hypothesis of a fast electrochemical reaction at the probe, and $\partial C^*/\partial y^* = 0$ at the impermeable wall of the channel (i.e. at $-0.005 < x^* < 0$ and at $0.01 < x^* < 0.015$). The concentration is assumed to be constant ($C^* = 1$) at the inlet ($x^* = -0.005$) and at the top boundary of the computational domain ($y^* = 0.005$), which for the flow conditions considered, are far enough from the probe, as it will be shown in next section. At $x^* = 0.015$ the conventional non-reflecting outflow boundary conditions for C^*, based on a discretized version of Eq. (2), were imposed.

$$S^* y^* \frac{\partial C^*}{\partial x^*} = \frac{1}{Re_\tau Sc}\left(\frac{\partial^2 C^*}{\partial y^{*2}}\right) \tag{2}$$

The computational domain sketched in Fig. 1 has been discretized with a non-uniform grid distribution. The grid nodes have been stretched towards the wall and towards the leading and trailing edges of the probe. Simulations of the time evolution of the averaged mass transfer rates over the probe using grids of 117×61 and 229×121 give the same frequency response to a sinusoidal modulated non-dimensional wall velocity gradient of the form

$$S^* = \overline{S}^* + A_S^* \sin(2\pi f^*) \tag{3}$$

with $\overline{S}^* = 150$ (i.e. $Re_\tau = 150$), $A^*S = 12.5$ and $f^* = 30$. The time-averaged Sherwood numbers, spatially averaged over the probe surface are 10.74 and 10.73 for the two grids. Consequently, the simulations have been carried out with the grid of 117×61 nodes.

4. Results and discussion

Fig. 3 shows the contours of the time-averaged concentration distribution and those of the fluctuations intensities of the concentration. The Leveque solution to the pseudo-steady-state equation (Eq. (4)), expressed in Eq. (5) is also shown for comparison.

$$\overline{S}^* y^* \frac{\partial \overline{C}^*}{\partial x^*} = \frac{1}{Re_\tau Sc}\left(\frac{\partial^2 \overline{C}^*}{\partial y^{*2}}\right) \tag{4}$$

$$\overline{C}^* = \frac{1}{\Gamma(4/3)}\int_0^\eta \exp(-q^3)\mathrm{d}q \tag{5}$$

where $\eta = y^*(\overline{S}^* Re_\tau Sc/9x^*)^{1/3}$ and Γ is the Gamma function

Eq. (4) can be obtained from the time-averaged version of Eq. (1) by dropping the time-averaged x-diffusion term and the turbulent transport term ($y\partial\langle s'c'\rangle/\partial)x$). Eq. (4) is based on the pseudo-steady-state assumption, which is valid for slowly varying velocity fields and, according to Hanratty and Campbell [1], it can be used to predict the time-averaged mass boundary layer for sufficiently small values of $s'/\langle S\rangle$.

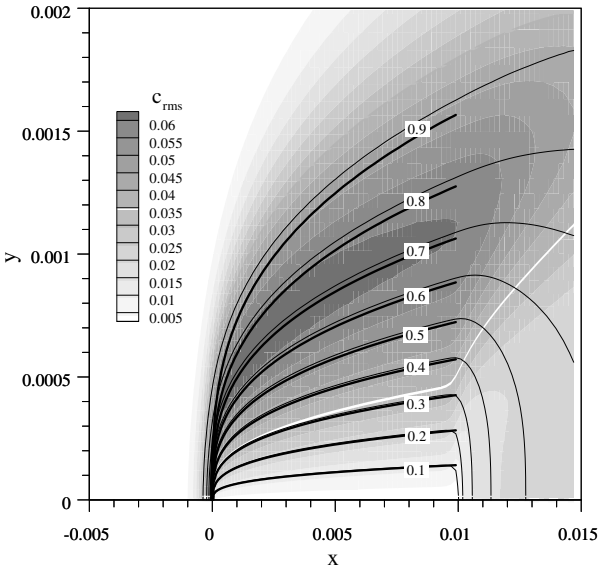

Fig. 3. Spatial distributions of the time-averaged concentration and fluctuation intensities.

It can be seen in Fig. 3, by comparing the numerical and the analytical results, that the end effects at the leading and trailing edge of the probe have a limited extension given the length of the probe considered ($L_p^+ = 1.5$). The numerical prediction of the mass transfer boundary closer to the wall (i.e. with a time-averaged concentration below 0.1) agrees with the analytical solution because of the low values of the fluctuation intensities of concentration. In fact, the time-averaged Sherwood number averaged over the probe predicted by the simulation is 10.56 and that obtained from the analytical solution is 10.57. The rms of the velocity gradient is 0.35, in agreement with the value of 0.36 reported by Jeon et al. [11] at $Re_\tau = 180$. The maximum value of the rms of the concentration is about 6 times smaller than the rms of S, as shown in Fig. 3, indicating the overall damping effect of the mass transfer boundary layer.

The time-averaged concentration distribution can be used to solve a linearized version of a transport equation for the fluctuations of concentration (Eq. (6)).

$$\frac{\partial c'^*}{\partial t^*} + \overline{S}^* y^* \frac{\partial c'^*}{\partial t^*} + s'^* y \frac{\partial \overline{C}^*}{\partial x^*} = \frac{1}{Re_\tau Sc}\left(\frac{\partial^2 c'^*}{\partial y^{*2}}\right) \tag{6}$$

Eq. (6) has been solved numerically by Fortuna and Hanratty [7] using Eq. (5) to compute $\overline{C}$ and assuming that the fluctuating velocity gradient can be written as a harmonic function, as

$$s'^* = \widehat{S}\exp(\mathrm{i}2\pi f^* t^*) \tag{7}$$

For $f^* \to 0$ the pseudo-steady-state approximation is

$$\frac{Sh'}{\langle Sh\rangle} = \frac{1}{3}\frac{s'}{\langle S\rangle} \tag{8}$$

The fluctuating velocity gradient and the fluctuating Sherwood number can be represented in terms of their spectral density functions (s.d.f.).

$$\langle Sh'^2\rangle = \int_0^\infty W_{Sh}\mathrm{d}f^* \tag{9}$$

$$\langle s'^2\rangle = \int_0^\infty W_S\mathrm{d}f^* \tag{10}$$

Fig. 4 shows the s.d.f. of the velocity gradient and the Sherwood number averaged over the length of the probe. It can be seen that the s.d.f. of the velocity gradient agrees with that reported by Jeon et al. [11] and that the damping effect of the mass transfer boundary layer is evident for $f^* > 5$. The relation of the s.d.f. of the velocity gradient and Sherwood number is shown in Fig. 5a. Note that the vertical scaling used in this figure is based on the result of the pseudo-steady-state approximation expressed by Eq. (8).

We solved Eq. (1) considering harmonic perturbations of the velocity gradient of the form indicated in Eq. (3) using the computational conditions described before. The amplitude of the sinusoidal perturbations is $A_S^* = 12.5$, which correspond to maximum intensities of the fluctuations of S^* of 8%. At this low amplitude, the response of

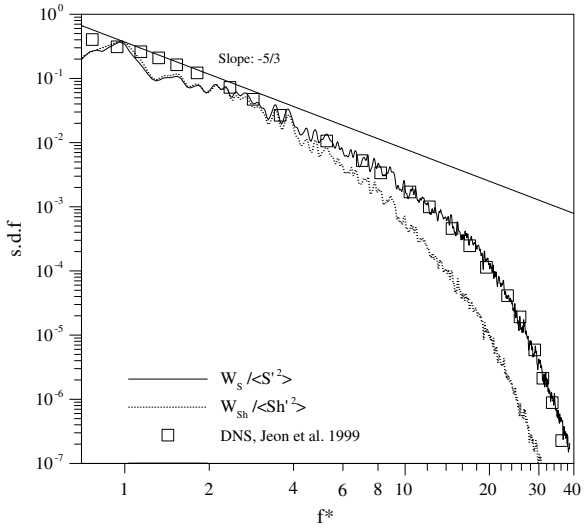

Fig. 4. Spectral density functions of the velocity gradient and Sherwood number.

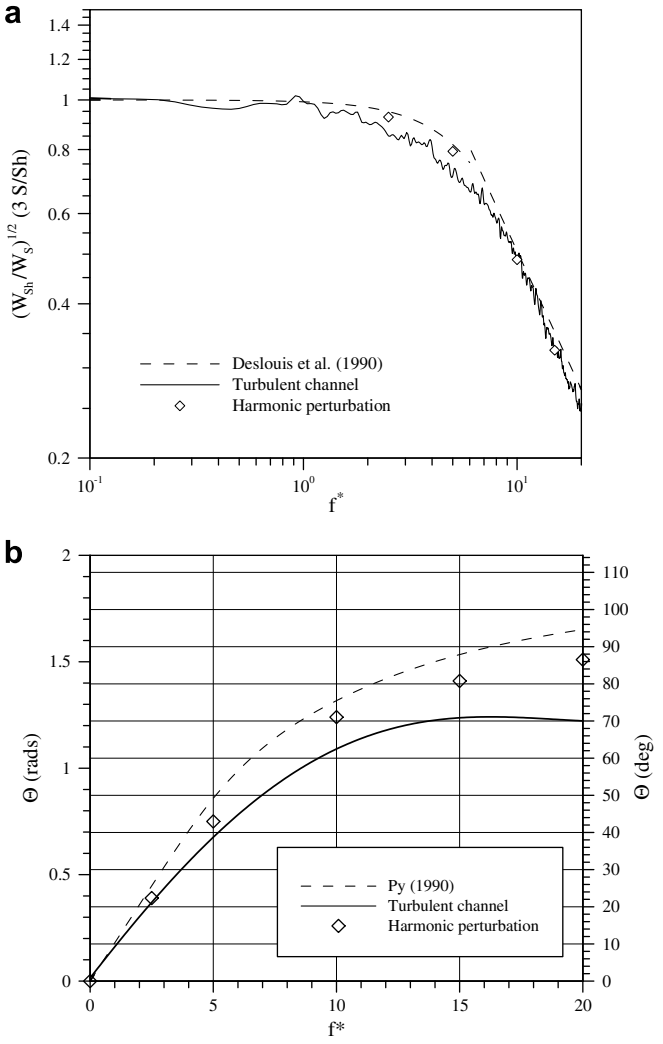

Fig. 5. Frequency response. (a) Ratio of the amplitudes of the fluctuations of the Sherwood number and the velocity gradient and (b) phase angles.

the averaged mass transfer rate only depends on the frequency and it is well reproduced by a sine function with a certain phase angle. It can be seen that the frequency response of the Sherwood number to a harmonic perturbations of the velocity gradient obtained from these numerical simulations agrees with the relations reported by Deslouis et al. [4] and plotted in Fig. 5a. As expected, at low frequencies ($f^* \leqslant 1$) the ratio of the amplitudes is well defined by the pseudo-steady-state solution (Eq. (8)). In the range $2 \leqslant f^* \leqslant 7$ the damping of the mass transfer boundary layer in a turbulent channel flow is underpredicted by the frequency response to harmonic perturbations of the wall shear stress as can be observed in Fig. 5a. The agreement between the response of the mass transfer rates to harmonic perturbations obtained with numerical simulations of Eq. (1) and the response based on the solution of the linearized equation for the fluctuations of concentration suggests that the response to turbulent fluctuations is sensitive to the fact that the wall stress signal has a range of frequencies instead of a single or a dominant one. The range of frequencies in which this effect is noticeable ($2 \leqslant f^* \leqslant 7$) corresponds to the inertial subrange of the s.d.f. of the wall shear stress (see Fig. 4).

The phase angle of the response of the mass transfer rates to the fluctuations of the wall shear stress is plotted in Fig. 5b. It can be seen that the solution of the linearized transport equation of the fluctuations of concentration (Eq. (6)) reported by Py [5] overpredicts the phase angle with respect to the numerical solution of the complete two-dimensional mass transfer equation (Eq. (1)) considering harmonic perturbations or turbulent fluctuations of the wall shear stress. The phase angle obtained with the wall shear stress of the turbulent channel flow in the range $f^* > 15$, in which the fluctuations have very low intensities (see Fig. 4), is approximately constant ($\theta \approx 70°$).

5. Conclusions

The response of a mass transfer probe to harmonic and turbulent fluctuations of the wall shear stress has been numerically predicted. While the response to harmonic perturbations agrees with the data existing in the literature, the response to turbulent fluctuations has a larger damping in comparison with that produced by harmonic fluctuations at moderate frequencies ($2 \leqslant f\delta/u_\tau \leqslant 7$). This indicates that the amplitude of the response of the wall shear stress in this range of frequencies which is within the inertial subrange of the power spectra is affected by the fact that the signal of the turbulent wall shear stress fluctuations has a specific distribution of energy among this range of frequencies. The phase angle of the response to fluctuations of the wall shear stress in a turbulent channel flow is lower in comparison with that of the harmonic fluctuations, specially at high frequencies. The differences between the observed response of the probe to the turbulent fluctuations and to the low-amplitude harmonic fluctuations can be attributed to the different amplitude and spectral characteristics of the two types of perturbations.

Acknowledgement

This study was financially supported by the Spanish Ministry of Science of Technology and FEDER under project DPI2006-0477.

References

[1] T.J. Hanratty, J.A. Campbell, Measurement of the wall shear stress, in: R.J. Goldstein (Ed.), Fluid Mechanics Measurements, second ed., Taylor and Francis, New York, 1996, pp. 575–648.
[2] T. Mizushina, The electrochemical method in transport phenomena, Adv. Heat Transfer 1 (1971) 87–159.
[3] R.D. Patel, J.J. McFeeley, K.R. Jolls, Wall mass transfer in laminar pulsatile flow in a tube, AIChE J. 21 (1975) 59–267.
[4] C. Deslouis, O. Gil, B. Tribollet, Frequency response of electrochemical sensors to hydrodynamic fluctuations, J. Fluid Mech. 215 (1990) 85–100.
[5] B. Py, Improvement in the frequency response of the electrochemical wall shear stress meter, Exp. Fluids 8 (1990) 281–285.
[6] J.E. Mitchell, T.J. Hanratty, A study of turbulence at a wall using an electrochemical wall stress meter, J. Fluid Mech. 26 (1966) 199–221.
[7] G. Fortuna, T.J. Hanratty, Frequency response of the boundary layer on wall transfer probes, Int. J. Heat Mass Transfer 14 (1971) 1449–1507.
[8] Z. Mao, T.J. Hanratty, Application of an inverse mass transfer method to the measurement of turbulent fluctuations in the velocity gradient at the wall, Exp. Fluids 11 (1991) 65–73.
[9] Z. Mao, T.J. Hanratty, Measurement of wall shear rate in large amplitude unsteady reversing flows, Exp. Fluids 12 (1992) 342–350.
[10] Z. Mao, T.J. Hanratty, Influence of large amplitude oscillations on turbulent drag, AIChE J. 40 (10) (1994) 1601–1610.
[11] S. Jeon, H. Choi, J.Y. Yoo, P. Moin, Space–time characteristics of the wall shear stress fluctuations in a low Reynolds number channel flow, Phys. Fluids 11 (1999) 3084–3094.
[12] A. Fabregat, Direct numerical simulation of the dispersion of buoyant plumes in turbulent channel flow, PhD Thesis, Universitat Rovira i Virgili, Tarragona, Spain, 2006.
[13] J. Pallares, A. Vernet, J.A. Ferré, F.X. Grau, Eduction of near-wall flow structures responsible for large deviations of the momentum-heat transfer analogy and fluctuations of wall transfer rates in turbulent channel flow, Comput. Fluids 35 (2007) 1327–1334.